INSTITUTE OF PHYSICS PUBLISHING JOURNAL OF OPTICS B: QUANTUM AND SEMICLASSICAL OPTICS

J. Opt. B: Quantum Semiclass. Opt. **6** (2004) 127–134 PII: S1464-4266(04)66608-0

Quantum feedback in a non-resonant cavity QED system

W P Smith and L A Orozco

Department of Physics and Astronomy, SUNY Stony Brook, Stony Brook, NY 11794-3800, USA

E-mail: Luis.Orozco@SUNYSB.EDU

Received 29 July 2003, accepted for publication 15 September 2003
Published 3 February 2004
Online at stacks.iop.org/JOptB/6/127 (DOI: 10.1088/1464-4266/6/2/002)

Abstract
Photon correlation measurements reveal the response of the conditional evolution of the cavity QED system to a novel quantum feedback protocol. A photodetection collapses the state of the system and triggers a feedback pulse with an adjustable delay and amplitude that alters the intensity driving the system. The conditional evolution of the system freezes into a new steady state where it resides until, after an amount of time determined by the experimenter, it re-equilibrates into the original steady state. We carry out a sensitivity analysis using a theoretical model with atomic detuning and make quantitative comparisons with measured results.

Keywords: cavity QED, quantum optics, quantum feedback

1. Introduction

Our cavity QED research focuses on the time evolution of quantum fluctuations both in the field [1, 2] and the intensity [3–6]. We work in the optical regime, where photodetectors are readily available to detect light which has been irreversibly emitted from the system. We use correlation functions to measure the non-classical properties of the field (squeezing) [7] and the intensity (antibunching and sub-Poissonian statistics) [4, 8] and focus on the time evolution of conditional states.

Once we have observed the time evolution of the conditional state of the system, the next step is to try to modify the evolution through quantum feedback triggered by the detection of a single photon.

In this paper we expand on our previous experimental results in a resonant cavity QED system for the application of feedback when the fluctuations are large compared with the mean [5, 6]. This is in contrast with previous work on quantum feedback where the fluctuations are small compared to the mean fields (see, for example, [9–11]). We explore the more general case of a cavity QED system where the cavity is not resonant with the driving field nor its two-level atoms and investigate the sensitivity of the system to atomic detuning, while keeping the detunings a few linewidths away from resonance. Section 2 describes the basic theoretical model. Section 3 describes the experiment which explores the general case of cavity and atomic detuning. Section 4 explores the sensitivity of the system to off-resonant excitation and section 5 presents our conclusions.

2. Theoretical model

One atom coupled to a single mode of the electromagnetic field of a cavity is a theoretically tractable problem [12]. The field and the atom couple through a dipole interaction with a strength given by

$$g = \sqrt{\frac{\mu^2 \omega_a}{2\hbar\epsilon_0 V}} \tag{1}$$

where $\mu = e\langle g|\mathbf{r}|e\rangle$ is the atomic transition dipole between two states, ω_a is the resonant transition frequency between states $|g\rangle$ and $|e\rangle$ and the electromagnetic field is quantized in a volume V.

We present results where the optical frequencies in the problem are not degenerate, $\omega_a \neq \omega_c \neq \omega_\ell$, where ω_c is the resonant frequency of the cavity and ω_ℓ is the frequency of the coherent drive. The Tavis and Cummings Hamiltonian with the appropriate drive and reservoirs in the rotating wave approximation describes this system.

The atom couples to modes other than the cavity mode and the cavity couples to modes outside the cavity. Master equation techniques permit the treatment of these couplings that lead to damping of the atomic inversion at a rate γ which is

the inverse of the lifetime of the excited atomic state, while the atomic polarization has a damping rate $\gamma_\perp$ for purely radiative decay $\gamma = 2\gamma_\perp$. The cavity decays with a rate $\kappa = c\,T/2L$, where T is the mirror transmissivity, and L is the length of the cavity. This light is collected in a detector and provides all of our information about the system. The detection of a photon collapses the state of the cavity, a process which affects the system itself. Finally, the system is driven externally with a field $\mathcal{E}/\kappa$, where $\mathcal{E}$ is the driving field amplitude (in units of $1/\mathrm{s}$).

The problem now includes the individual atomic and cavity energies, the coherent coupling g, the damping rates and the driving field. Two arrangements of the various rates in the problem were first standardized in optical bistability [13]: the single-atom cooperativity, $C_1 = g^2/\kappa\gamma$, scales the influence of a single atom in the system. The saturation photon number, $n_0 = \gamma^2/3g^2$, approximates the number of photons necessary to saturate the atoms in a Fabry–Perot cavity. In optical bistability this is the value of the intra-cavity intensity necessary to take the system to the upper branch. For N atoms in the system the cooperativity simply scales, $C = C_1 N$. The strong coupling regime of cavity QED requires $n_0 \leqslant 1$ and $C_1 \geqslant 1$. In our experiment $g \approx \gamma \approx \kappa$, touching the strong coupling regime.

2.1. Quantum case

With weak driving, the system can be accurately modelled with a basis that includes up to two excitations of the coupled normal modes of the field and the atoms [14, 15]. In this regime, photodetections are very infrequent and the state before a detection can be taken to be the steady state, which is almost pure:

$$|\psi_{\mathrm{ss}}\rangle = |0, G\rangle + \alpha\left(|1, G\rangle - \frac{2g\sqrt{N}}{\gamma}|0, E\rangle\right) + \alpha^2\left(\zeta_0\frac{1}{\sqrt{2}}|2, G\rangle - \xi_0\frac{2g\sqrt{N}}{\gamma}|1, E\rangle\right) + \cdots. \tag{2}$$

Here $|n, G\rangle$ represents n photons with all (N) atoms in their ground state, $|n, E\rangle$ represents n photons with one atom in the excited state with the rest $(N-1)$ in their ground state, symmetrized over all atoms. The small parameter is $\alpha = \langle\hat{a}\rangle = \mathcal{E}/[\kappa(1 + C_1 N)]$, which depends on the input driving field $\mathcal{E}$, while ζ_0 and ξ_0 are coefficients of the order of unity for the two-excitation components that have nonzero photon number and depend on g, κ and γ [14, 15].

After a photodetection occurs $|\psi_{\mathrm{ss}}\rangle$ collapses to $\hat{a}|\psi_{\mathrm{ss}}\rangle/\sqrt{\langle\hat{a}^\dagger\hat{a}\rangle_{\mathrm{ss}}}$ which evolves as the conditioned state:

$$|\psi_{\mathrm{c}}(\tau)\rangle = |0, G\rangle + \alpha\left(\zeta(\tau)|1, G\rangle - \xi(\tau)\frac{2g\sqrt{N}}{\gamma}|0, E\rangle\right) + \mathrm{O}(\alpha^2). \tag{3}$$

This is different from the initial state because ζ (the 'field' evolution) and ξ (the 'atomic polarization' evolution) oscillate coherently at the vacuum Rabi frequency $\Omega = \sqrt{g^2 N - (\kappa - \gamma/2)/2}$ over time as the system re-equilibrates, exchanging energy between the atomic polarization and the cavity field [14, 15].

2.2. Correlation measurements

We take an operational approach to correlations functions: a photodetection collapses the steady state system, $|\psi\rangle_{\mathrm{ss}}$, into the same conditioned state, $|\psi\rangle_{\mathrm{c}}$, every time. This allows us to collect measurements of many individual realizations of the same system. Conditional quantum states can be measured using $g^{(2)}(\tau)$, the intensity correlation function. $g^{(2)}(\tau)$ has been described for a general quantum optical source[16] and specifically for our cavity QED source [4]. Here we only list the relevant properties. The normalized correlation function of the intensity is the time-ordered and normally ordered average:

$$g^{(2)}(\tau) = \frac{\langle\psi_{\mathrm{ss}}|\hat{a}^\dagger(t)\hat{a}^\dagger(t+\tau)\hat{a}(t+\tau)\hat{a}(t)|\psi_{\mathrm{ss}}\rangle}{\langle\psi_{\mathrm{ss}}|\hat{a}^\dagger(t)\hat{a}(t)|\psi_{\mathrm{ss}}\rangle^2} \tag{4}$$

$$= \frac{\langle\psi_{\mathrm{c}}|\hat{n}(t+\tau)|\psi_{\mathrm{c}}\rangle}{\langle\psi_{\mathrm{ss}}|\hat{n}(t)|\psi_{\mathrm{ss}}\rangle}, \tag{5}$$

where $\hat{n} = \hat{a}^\dagger\hat{a}$. A $g^{(2)}(\tau)$ measurement records the likelihood that a photon will be emitted from the system *after* one photon has already been detected, normalized by the photodetection rate in the steady state. Photodetections a long time after one photon has been detected, $\tau \gg \tau_{\mathrm{char}}$, are uncorrelated with the original photodetection, where $\tau_{\mathrm{char}} = 2/(\gamma_\perp + \kappa)$ is a characteristic time dictated by the average of the decay rates in the system. Experimentally, we take this to be our steady state. At short times $\tau \approx \tau_{\mathrm{char}}$ we can observe the conditional dynamics of the system.

2.3. Cavity QED with quantum feedback

The cavity field evolution, $\zeta(\tau)$, and the atomic dipole evolution, $\xi(\tau)$, oscillate coherently at the vacuum Rabi frequency Ω. There are times when—due to the natural system dynamics—these coefficients are equal. If we choose one of these times $\tau = T$ such that $\zeta(T) = \xi(T)$ then, to order α, we obtain [5]

$$|\psi_{\mathrm{c}}(T)\rangle \simeq |0, G\rangle + \alpha'\left(|1, G\rangle - \frac{2g\sqrt{N}}{\gamma}|0, E\rangle\right). \tag{6}$$

At these special times the state of the system is of the form of the steady state $|\psi_{\mathrm{ss}}\rangle$ but with a different mean field $\alpha' = \zeta(T)\alpha$ [5]. The system, however, is not actually in a steady state at this time. The external field $\mathcal{E}$ is driving the system towards the original steady state, given by α. The system drive is the only system parameter that, at time T, does not meet the steady state criteria. The conditional state can be stabilized if, at time T, we change to $\mathcal{E}'$, corresponding to the steady state cavity field, α'. Then the system will reside in the new steady state given by equation (6).

This way of stabilizing the conditional state is possible because it is a pure quantum state with two real parameters (ζ and ξ) and two control parameters (the size and parity of the change in drive $\alpha' - \alpha$ and the timing of the change T). Ordinarily, $g^{(2)}(\tau)$ would always be symmetrical in τ by construction. If this detection is used to trigger a feedback pulse on the system, however, the correlation function will no longer be time-symmetric. Nevertheless, for $\tau > 0$ the expression (5) still measures the conditioned (c) state in the presence of feedback (fb):

$$g^{(2)}(\tau) \simeq \frac{|\langle 1, 0|\psi_{\mathrm{c+fb}}(\tau)\rangle|^2}{|\langle 1, 0|\psi_{\mathrm{ss}}\rangle|^2} = [\zeta_{\mathrm{fb}}(\tau)]^2. \tag{7}$$

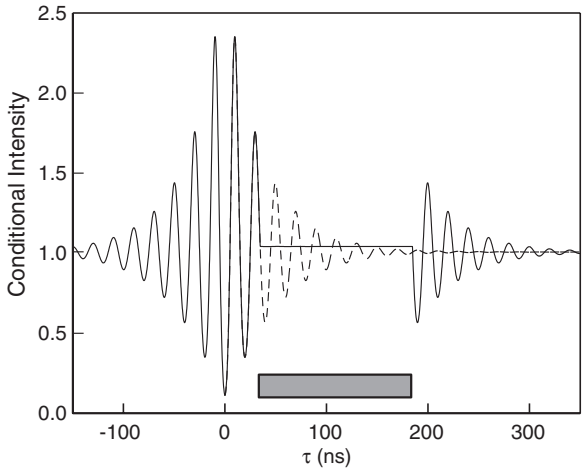

Figure 1. Intensity correlation function with (full curve) and without (broken curve) quantum feedback. The grey box indicates the application time of the square feedback pulse, $T = 34.7$ ns, $\delta I = +1.7\%$. The system resides in the new steady state for 150 ns before the driving intensity is returned to its original value. Notice that the new steady state is higher than the original. $\Omega/2\pi = 50$ MHz, $\kappa/2\pi = 4.9$ MHz and $\gamma_\perp/2\pi = 3.0$ MHz.

Figure 1 shows the predicted intensity correlation with the quantum feedback. The change in the intensity needed for stabilization is $\delta I = |\alpha' - \alpha|^2/|\alpha|^2 = 0.017$ at a time $T = 34.7$ ns. The system resides in the new steady state for 150 ns before the driving intensity is returned to its original value. The system then re-equilibrates into the original steady state. This feedback protocol captures the dynamic evolution and then releases it with the exact phase and amplitude that it had at a later time.

2.4. Detunings in cavity QED and a semi-classical model

The atomic polarization can be treated as a harmonic oscillator in the weak-field limit, when most of the atoms are in the ground state [17]. A single electromagnetic mode of a Fabry–Perot cavity ($\hat{\mathcal{A}}$, $\hat{\mathcal{A}}^\dagger$) and a collective atomic dipole ($\hat{\mathcal{S}}_-$, $\hat{\mathcal{S}}_+$, $\hat{\mathcal{S}}_z$) can be modelled as coupled harmonic oscillators with loss rates κ and $\gamma_\perp$ that couple together with strength, g.

This description of the system is motivated from the equations of motion for the system from master equation techniques. Assuming the atoms and field are decorrelated $\langle \hat{S}_z \hat{a}\rangle = \langle \hat{S}_z\rangle\langle \hat{a}\rangle$, and making the rotating wave approximation gives us the Maxwell–Bloch equations [18]:

$$\langle \dot{\hat{\mathcal{A}}}\rangle = -[\kappa + \mathrm{i}(\omega_\mathrm{c} - \omega_\ell)]\langle \hat{\mathcal{A}}\rangle + g\langle \hat{S}_-\rangle + \mathcal{E} \tag{8}$$

$$\langle \dot{\hat{\mathcal{S}}}_-\rangle = -[\gamma_\perp + \mathrm{i}(\omega_\mathrm{a} - \omega_\ell)]\langle \hat{\mathcal{S}}_-\rangle + 2g\langle \hat{S}_z\rangle\langle \hat{\mathcal{A}}\rangle \tag{9}$$

$$\langle \dot{\hat{S}}_z\rangle = -\gamma\left(\langle \hat{S}_z\rangle + \frac{N}{2}\right) - g\langle \hat{\mathcal{A}}^\dagger\rangle\langle \hat{\mathcal{S}}_-\rangle - g\langle \hat{\mathcal{S}}_+\rangle\langle \hat{\mathcal{A}}\rangle \tag{10}$$

and the complex conjugates of equations (8) and (9).

We have assumed that the laser and the cavity are locked to the atomic resonance, $\omega_\ell = \omega_\mathrm{c} = \omega_\mathrm{a}$. Detunings can arise as a result of the experimental conditions, or can be introduced intentionally by the experimenter.

The theory of detunings and N atoms coupled to a cavity mode is treated extensively by Brecha *et al* [19]. Detunings are handled within the master equation and the Maxwell–Bloch equations (8)–(10) by redefining the decay rates [19]:

$$\kappa \to \kappa(1 + \mathrm{i}\Theta) \equiv \tilde{\kappa} \tag{11}$$

$$\gamma_\perp \to \gamma_\perp(1 + 2\mathrm{i}\Delta) \equiv \tilde{\gamma}_\perp \tag{12}$$

where $\Theta = (\omega_\mathrm{c} - \omega_\ell)/\kappa$ and $\Delta = (\omega_\mathrm{a} - \omega_\ell)/\gamma_\perp$. The Maxwell–Bloch equations are now

$$\langle \dot{\hat{\mathcal{A}}}\rangle = -\tilde{\kappa}\langle \hat{\mathcal{A}}\rangle + g\langle \hat{\mathcal{S}}_-\rangle + \mathcal{E} \tag{13}$$

$$\langle \dot{\hat{\mathcal{A}}}^\dagger\rangle = -\tilde{\kappa}^\star\langle \hat{\mathcal{A}}^\dagger\rangle + g\langle \hat{\mathcal{S}}_+\rangle \tag{14}$$

$$\langle \dot{\hat{\mathcal{S}}}_-\rangle = -\tilde{\gamma}_\perp\langle \hat{\mathcal{S}}_-\rangle + 2g\langle \hat{S}_z\rangle\langle \hat{\mathcal{A}}\rangle \tag{15}$$

$$\langle \dot{\hat{\mathcal{S}}}_+\rangle = -\tilde{\gamma}_\perp^\star\langle \hat{\mathcal{S}}_+\rangle + 2g\langle \hat{S}_z\rangle\langle \hat{\mathcal{A}}^\dagger\rangle \tag{16}$$

$$\langle \dot{\hat{S}}_z\rangle = -2\gamma_\perp\left(\langle \hat{S}_z\rangle + \frac{N}{2}\right) - g\langle \hat{\mathcal{A}}^\dagger\rangle\langle \hat{\mathcal{S}}_-\rangle - g\langle \hat{\mathcal{S}}_+\rangle\langle \hat{\mathcal{A}}\rangle \tag{17}$$

where the input field $\mathcal{E}$ drives only $\langle \hat{\mathcal{A}}\rangle$. We assume that the cavity mode is constant in intensity throughout the cavity. In the weak field limit, Xiao *et al* [20] showed that calculations, such as correlations, using the quantum regression theorem are independent of the mode function of the cavity. Considering the steady state, $\langle \dot{\hat{\mathcal{A}}}\rangle = \langle \dot{\hat{\mathcal{S}}}_-\rangle = \langle \dot{\hat{S}}_z\rangle = 0$, we can obtain an equation relating the cavity field to the drive—up to factors involving (g, κ, γ). We find $\mathcal{E} \propto \langle \hat{\mathcal{A}}\rangle[1+1/(1+|\langle \hat{a}\rangle|^2)]$, which is nonlinear unless $\langle \hat{a}\rangle \ll 1$. In this weak field case the steady state becomes

$$\langle \hat{\mathcal{A}}\rangle^\mathrm{ss} = \alpha = \frac{\mathcal{E}}{\tilde{\kappa}(1+2C)}, \qquad \langle \hat{\mathcal{S}}_-\rangle^\mathrm{ss} = \beta = -\alpha\frac{2\sqrt{N}g}{\tilde{\gamma}}. \tag{18}$$

These are the same steady state values found in the fully quantum mechanical calculation [14, 15].

If, as before, we assume that most of the atoms are in the ground state, then the expectation value of the population operator becomes $\langle \hat{S}_z\rangle = -\sqrt{N}/2$ and $\langle \dot{\hat{S}}_z\rangle = 0$. The equations now reduce to those describing the interaction of classical oscillators, with one oscillator to describe the atomic dipole and the other to describe the field within the cavity:

$$\langle \dot{\hat{\mathcal{A}}}\rangle = -\tilde{\kappa}\langle \hat{\mathcal{A}}\rangle + \sqrt{N}g\langle \hat{\mathcal{S}}_-\rangle + \mathcal{E} \tag{19}$$

$$\langle \dot{\hat{\mathcal{A}}}^\dagger\rangle = -\tilde{\kappa}^\star\langle \hat{\mathcal{A}}^\dagger\rangle + \sqrt{N}g\langle \hat{\mathcal{S}}_-^\dagger\rangle \tag{20}$$

$$\langle \dot{\hat{\mathcal{S}}}_-\rangle = -\tilde{\gamma}_\perp\langle \hat{\mathcal{S}}_-\rangle + \sqrt{N}g\langle \hat{\mathcal{A}}\rangle \tag{21}$$

$$\langle \dot{\hat{\mathcal{S}}}^\dagger{}_-\rangle = -\tilde{\gamma}_\perp^\star\langle \hat{\mathcal{S}}_-^\dagger\rangle + \sqrt{N}g\langle \hat{\mathcal{A}}^\dagger\rangle. \tag{22}$$

These are the weak field limit semi-classical Maxwell–Bloch equations.

Missing from this model is the quantum jump in the state of the system upon a photodetection. A photodetection in our detector collapses the wavefunction of the system. Although the jump is not described by the differential equations, we can use them to find the steady state of the system, use the measured value of $g^{(2)}(0) = \zeta_0^2$ (see equation (7)) to find the cavity field jump and then infer the jump in atomic dipole [14]. These values then become the initial conditions for the fields after the wavefunction collapses. The differential equations then model the evolution of the fields back to the steady state.

We have used this procedure to obtain the theoretical prediction of figure 1. The jump in the atomic dipole is small compared with the field jump. It shifts the phase of the two fields with respect to one another.

A cavity QED system subjected to a step excitation undergoes an oscillatory exchange of energy between the atoms and cavity before it reaches the steady state [21, 22]. This exchange is the time-domain analogue of the vacuum-Rabi doublet which has been observed in the transmitted spectrum [23–26]. Previous research has focused on step excitations from the steady state which extinguish the drive, or turn-on steps from no drive. The steps in this work are between two non-zero steady states and are applied when a photodetection alerts us to the timing of the oscillatory exchange between atoms and cavity.

When the system is resonant only one field quadrature is excited. In general, when there is detuning in the system both quadratures of the cavity field are excited. This degrades the ability of the current feedback protocol, since now four feedback parameters are required to fully control the system.

2.5. Refinements of the model

A beam of thermal atoms travelling through the cavity introduces a number of complications [27–29], many of which have been discussed for our experiment [4]. The coupling rate g defined in equation (1) is for an atom coupled to an anti-node of the cavity standing wave. The atoms are moving, however, and a spatially dependent coupling constant, $g(\mathbf{r}_j)$, describes the interaction of each of the atoms with the Gaussian waist of the cavity. Also, a moving atom crossing a cavity mode sees the cavity as a pulse of light. For this reason, the atoms see a spectrally broadened cavity mode, an effect called transit broadening.

There is a Doppler velocity distribution along the direction of the beam which couples to the cavity mode because of the angular spread defined by the collimating slits. This inhomogeneous effect yields a spread of atomic detunings within the cavity. There are also Poissonian atom number fluctuations within the thermal atomic beam, which affects the oscillation frequency Ω.

The theoretical method described for dealing with detunings is similar to that of [4]. It allows us to use values determined from the apparatus for the three rates $(g, \kappa, \gamma_\perp)$ in the system along with the Maxwell–Bloch equations to model the data.

To model this inhomogeneous effect we begin by taking the initial value of the cavity field h after a photodetection [15, 19]:

$$h(\tau = 0) = 1 - \frac{2\tilde{C}}{N}\,\frac{\tilde{\mu}}{\tilde{\mu}+1}\,\frac{2\tilde{C}}{1+2\tilde{C}} \tag{23}$$

with $\tilde{\mu} = 2\tilde{\kappa}/\tilde{\gamma}$ and $\tilde{C} = Ng^2/\tilde{\kappa}\tilde{\gamma}$. The evolution of the cavity field and atomic dipole are given by equations (19) and (21). We compute the field inside the cavity for a range of individual detunings. These fields are averaged and the resulting field is squared to find the intensity.

A similar method describes a drift of the cavity lock. The field evolution within the cavity is calculated for a range of cavity detunings and the fields are added. Combining both detunings, the evolution is computed at each value of Δ for each value of Θ. We reach quantitative agreement to better than 20% with this approach [4].

3. Experiment

The apparatus consists of a high-finesse optical cavity, which is driven by and locked to a cw excitation laser. The laser is locked to a ^{85}Rb resonance at 780 nm with a saturation spectroscopy technique. A collimated thermal beam of ^{85}Rb atoms interacts with the cavity mode. Avalanche photodiodes (APD) detect the light emitted from one side of the cavity and produce signals which travel to a time-to-digital converter (TDC) to make correlation measurements.

The procedure consists of optimizing the system to produce a non-classical correlation, then feeding back—after pulse shaping—the electronic pulses from the conditioning photodetections to an EOM before the cavity entrance to alter the intensity of the driving light. We have previously shown that this feedback protocol can project the system into a steady state [5]. We then explore the sensitivity of the suppression to the atomic detuning in the system by locking the cavity at a different frequency than the atomic resonance.

3.1. Cavity QED system and intensity correlator

The apparatus and experiment has been described in detail in [4, 6], but we summarize here the basic components and those relevant to the system detunings. The cavity defines a TEM_{00} mode with two mirrors with different transmission coefficients, $T_1 = 15$ ppm and $T_2 = 300$ ppm. The input transmission is smaller than the output to ensure that most of the signal escapes from the cavity on the detector side. A typical cavity finesse for this arrangement is $\mathcal{F} \approx 21\,000$. Two cylindrical piezo-electric-transducers (PZT) control the length of the cavity.

The lock and signal beams have orthogonal linear polarizations when combined at a beamsplitter before the cavity entrance. They are projected into opposite circular polarizations before entering the cavity and the reflected lock beam produces the error signal for cavity locking. We chop the lock beam before it is inserted into the cavity. One lock cycle consists of a period of 600 μs during which the cavity is actively locked, followed by a period of 350 μs during which the cavity is 'freely evolving'. We estimate the quality of the lock by observing whether the cavity transmission is constant, particularly at the beginning and ending of a lock cycle. The cavity drifts preferentially in one direction. This is because there is always a thermal drift from the liquid-nitrogen-cooled copper finger which surrounds the cavity to reduce background vapour. The cavity lock is usually better than $\Theta < 0.10$, although if the system is far from thermal equilibrium the large amount of drift due to the cold finger causes the limit to be closer to $\Theta < 0.50$.

The lock and signal beams are both derived from a Coherent Verdi-5 pumped Ti:sapphire 899-01, which is locked using an RF saturation spectroscopy measurement. A double passed acousto-optic modulator (AOM) adjusts the signal and lock beam frequencies around atomic resonance, which allows us to compensate for Doppler detunings or to explore the effect of laser–atom detuning.

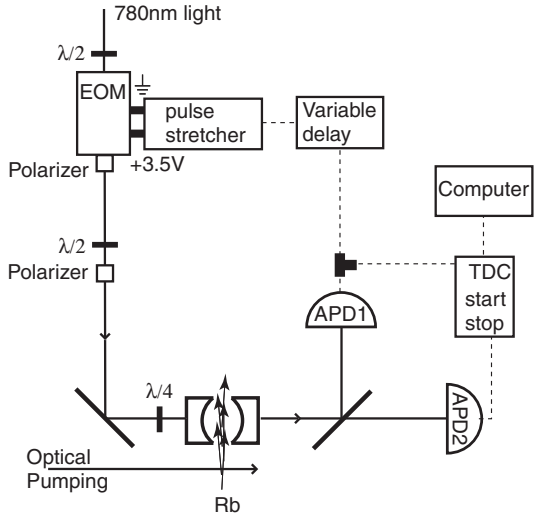

Figure 2. Simplified diagram of the experimental set-up. A collimated thermal beam of optically pumped Rb atoms traverses an optical cavity. Intensity correlations are measured with two avalanche photodiodes (APD), gating electronics, a time-to-digital converter (TDC) and a histogramming memory and computer. Photo-detections at APD1 are used to trigger a change in the intensity injected into the cavity. Optics shown are relevant for control of the size of the intensity step and the polarization of the light injected into the cavity.

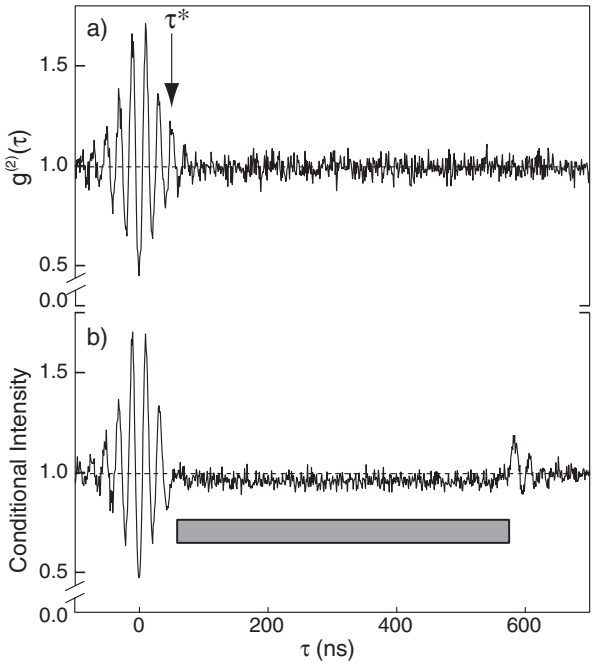

Figure 3. Resonant intensity correlation measurements with and without quantum feedback, $\Delta = \Theta = 0$. τ^* indicates the peak targeted for suppression with feedback. $\Omega/2\pi = 49$ MHz, data binned into 1.0 ns bins. (a) Typical measured $g^{(2)}(\tau)$. (b) Measured intensity correlation function with quantum feedback in a resonant system. $\Delta I = -2.7\%$, $\tau_{\rm fb} = 45$ ns. The grey box indicates the 500 ns application time of the square feedback pulse.

Our system is in the intermediate regime of cavity QED, where $g \approx (\kappa, \gamma)$. Typical rates are $(g, \kappa, \gamma)/2\pi = (6.1, 4.9, 6.0)$ MHz. $C_1 = 1.3$ is typical for our system.

An oven located 35 cm from the cavity produces a thermal beam of Rb atoms, at a typical temperature of 460 ± 0.1 K, by chopping the current in the resistive wire at about 0.1 Hz. Several slits collimate the atomic beam to a spread of 2.8 mrad. A diffusion pump and a liquid-nitrogen-cooled copper sleeve produce a typical operating pressure of about 5×10^{-7} Torr.

An atom–cavity detuning is a consequence of using a thermal atomic beam as an atom source for the cavity. Aligning the atomic beam perfectly perpendicular to the cavity mode is challenging. Angles up to 20 mrad are common. With typical atomic beam velocities, an angle of 10 mrad implies a shift of about $\mathbf{k} \cdot \mathbf{v}/2\pi \approx 5$ MHz. With this small detuning, and the large amount of power in the optical pumping beam, the optical pumping efficiency is unchanged. The atom–cavity detuning is compensated for via the previously mentioned AOM.

A 5 G magnetic field which is collinear to the cavity axis to within 40 mrad provides the quantization axis for optical pumping and creation of a beam of two-level atoms. ($5S_{1/2}$, $F = 3$, $m_F = 3 \rightarrow 5P_{3/2}$, $F' = 4$, $m'_F = 4$ transition of ^{85}Rb at 780 nm with $\gamma/2\pi = 6.07$ MHz).

The light escaping the cavity is detected by two avalanche photodiodes (APD) located behind a 50/50 beamsplitter, see figure 2. The transistor–transistor logic (TTL) signals of the photodiodes are sent through gating electronics, and ultimately to a computer, to produce intensity–intensity correlations. The pulse of APD1 is split and one copy is sent to a pulse stretcher and electro-optic modulator (EOM)/polarizer pair to alter the intensity of the drive.

The feedback information is derived from the TTL produced by APD1. The TTL from the start detector proceeds through a power splitter, a variable delay (0.5–32 ns) and then to a pulse stretching circuit. After a short delay, the circuit produces a longer pulse. Due to the optical and electronic delays in the system, the minimum feedback time is $\tau_{\rm fb} = 43$ ns. The output of the circuit is directly applied to a Gsänger model LM0202P-IR5W EOM with an output polarizer attached. Optical intensity steps are produced when the voltage is applied to the EOM/polarizer.

3.2. Intensity-correlation measurements

The data-taking procedure begins by recording correlation functions without feedback. We begin by aligning the optical pumping beam to ensure that we have two-level atoms. Then we determine the $\Delta = 0$ condition for the system. The ratio of normalized input ($Y = |\mathcal{E}|^2/(\kappa^2 n_0)$) to normalized transmitted ($X = |\alpha|^2/n_0$) intensities including cavity–laser detuning is given by [13]

$$\frac{Y}{X} = \left|\left(1 + \frac{2C}{1+\Delta^2}\right) + \mathrm{i}\left(\Theta - \frac{2C\Delta}{1+\Delta^2}\right)\right|^2 \qquad (24)$$

and is a minimum for $\Delta = 0$ and $\Theta = 0$. Once we have located the laser frequency which minimizes the transmitted intensity, we determine the frequency of the laser which minimizes $g^{(2)}(0)$. Several more measurements at various intensities determine the drive for the weak field regime. We then optimize the feedback routine to achieve the best suppression of the system's oscillation [5, 6].

Figure 3(a) depicts a typical $g^{(2)}(\tau)$ measurement. A photon is emitted from the cavity at $\tau = 0$, disturbing the

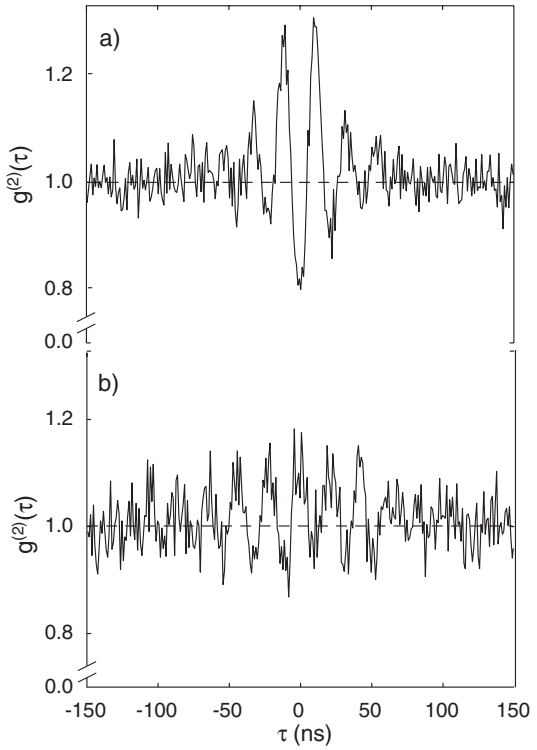

Figure 4. Measured $g^{(2)}(\tau)$ with atom–cavity detuning. Compare with the resonant $g^{(2)}(\tau)$ shown in figure 3(a), which has the same system parameters. (a) $\Delta = 0.7$, the antibunching has degraded with respect to the resonant case although the time-delayed Schwarz inequalities are still violated. (b) $\Delta = 2.3$. The signal is now bunched and super-Poissonian, $g^{(2)}(\tau = 0) = 1.11 \pm 0.04$.

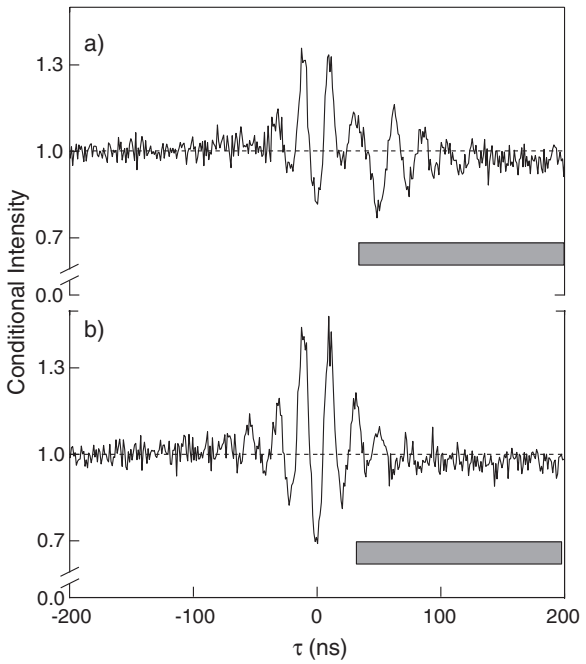

Figure 5. Measured intensity correlation functions with atom–cavity detuning and quantum feedback. (a) $\Delta = -0.7$, (b) $\Delta = +0.7$. The grey box corresponds to the region with the feedback pulse, while system parameters are identical to those in figure 3.

steady state of the system. $\tau = 0$ is defined by a photodetection in APD1: we then histogram the subsequent arrival times of photodetections in APD2. The system then exchanges any remaining energy between the cavity mode and atoms at the coupling frequency, Ω. At any time during this exchange, the system can lose this excitation through either atomic spontaneous emission or through a cavity emission. Without a feedback step, our driven coupled system again resides in the steady state after some characteristic time dictated by an average of the loss rates, $(\kappa+\gamma_\perp)/2$. This evolution can be seen in the correlation function in figure 3(a). This correlation is sub-Poissonian ($g^{(2)}(\tau = 0) = 0.46 \pm 0.03$) and antibunched (positive curvature at $\tau = 0$).

Figure 3(b) depicts an intensity correlation measurement with feedback for the same system parameters as figure 3(a). The feedback step size is $\Delta I = -2.7\%$ and the system is held in the new steady state for 500 ns before it is released. It then exchanges energy at the vacuum-Rabi frequency as it re-equilibrates into the original steady state.

We now explore the effects of the cavity–atom detuning, Δ, defined in equation (12). In a resonant system only one cavity field and one atomic dipole quadrature is excited, and a $g^{(2)}(\tau)$ measurement provides intensity information about that quadrature. When both quadratures are excited the resulting $g^{(2)}(\tau)$ is a combination of both. Figure 4 shows two $g^{(2)}(\tau)$ measurements for a detuned system $\Delta \neq 0$. For small detunings, $\Delta < 1$, the antibunching degrades, as shown in figure 4(a). The correlation function is nearly flat when $\Delta = 1$ [4] and re-appears again for $\Delta > 1$ but with classical statistics, see figure 4(b).

3.3. Correlation measurements with detuning and quantum feedback

The feedback suppression degrades with detunings present in the system, as shown in figures 5 and 6. Each quadrature of the cavity field requires feedback at the correct time with the appropriate amplitude. Hence four parameters are required when both quadratures are excited. One EOM producing an intensity step at a specified time (two parameters) is not sufficient to halt the system evolution in this case. For this measurement a cavity detuning is present and we place a limit to it of $|\Theta| \leqslant 0.5$.

Figure 5 has a small atomic detuning (± 0.7) and the field is antibunched and sub-Poissonian. The case of positive detuning shows closer behaviour to the resonant excitation. This is related to the compensation of atomic and cavity detuning that exists when the two detunings are equal [19].

Figure 6 shows the conditional intensity in the presence of a large atomic detuning for the two signs of the detuning. The system displays bunching and is super-Poissonian, so it looks as if it is classical; however, in this regime it still shows squeezing [30]. The asymmetry in the response for the two values of Δ comes from the presence of cavity detunings $|\Theta| < 0.5$.

4. Sensitivity analysis

We have followed the response of the system to different step amplitudes when the optimal suppression occurs at a stronger drive than the original steady state. Figure 7 illustrates the

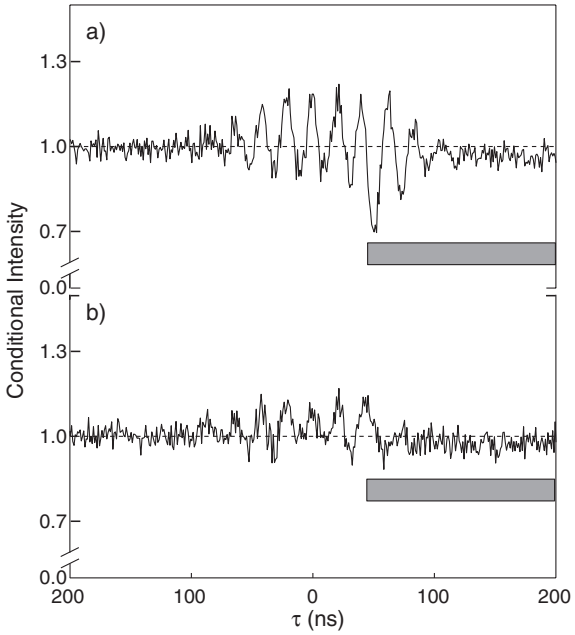

Figure 6. Measured intensity correlation functions with atom–cavity detuning. Compare with the resonant $g^{(2)}(\tau)$ shown in figure 3(a). The grey box corresponds to the region with the feedback pulse, while system parameters are identical to those in figure 3. (a) $\Delta = -2.0$, (b) $\Delta = +2.0$.

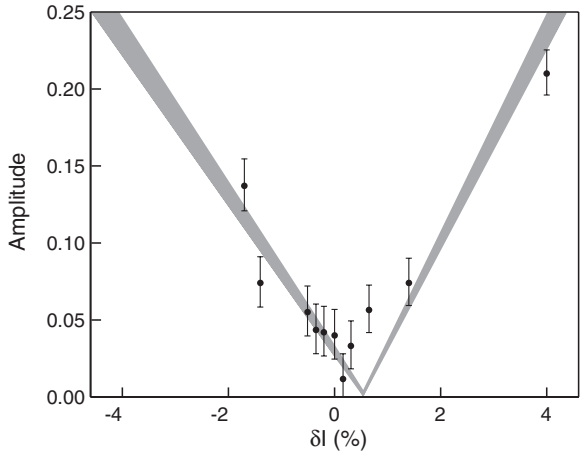

Figure 7. Response of the system to feedback intensity steps of various sizes. For this parameter set, the optimal suppression occurs at $\Delta I = +0.2\%$. The grey area is a model prediction which includes the rise time of the intensity step and a range of detunings of the system.

sensitivity of the system to the feedback amplitude when a positive step freezes the oscillation. The model includes the 7 ns rise time of the intensity step. The grey area represents the model prediction region for a range of detunings. The model includes a cavity–atom detuning from $\Delta = 0$ (resonance) up to $\Delta = 0.3$ to reflect the previously mentioned uncertainty in determining $\Delta = 0$. A cavity–laser detuning from resonance up to $\Theta = 0.5$ models the unstable cavity lock during that particular data set. Although the data are consistent with a completely suppressed oscillation (at $\Delta I = 0.2\%$) the trend of the data points does converge at zero. The best linear fit to the two individual arms of the V-shaped data has a minimum at an amplitude of 0.02. The detunings make perfect feedback impossible and slightly lift the minimal amplitude of the model above zero.

To quantify the amount of feedback suppression we make correlation measurements at several values of cavity–atom detuning, take a fast Fourier transform and compare the power in the correlation function during the time the feedback pulse is applied, with and without the feedback. The power enhancement in the $g^{(2)}(\tau)$ is computed with a MATLAB FFT routine and is given by

$$P(f_k) = \frac{\left|\sum_{\tau_j=\tau_{\rm fb}}^{\tau_{\rm N}} g^{(2)}(\tau_j)\omega_N^{\tau_{j-1}f_{k-1}}\right|}{\left|\sum_{\tau_j=\tau_{\rm fb}}^{\tau_{\rm N}} g^{(2)}(-\tau_j)\omega_N^{\tau_{j-1}f_{k-1}}\right|} \qquad (25)$$

where $\omega = \mathrm{e}^{(-2\pi \mathrm{i}/N)}$. We compute the power in the correlation measurement when the feedback pulse is applied and normalize it by the power in the same region of the correlation measurement for negative times. With no feedback, the power in the positive and negative times is equal. The data are acquired over a 1 μs interval and are divided into 2000 500 ps bins. 48 bins are added to make a power of 2 in the bins. Normalizing the power by the negative times allows one to see the suppression or enhancement of the power during the feedback as compared to the power in the absence of feedback.

Notice that the power ratio peaks at some value of the detuning and then lowers again. This is because, as the detuning is increased, the power in the intensity correlation function is also changing, as shown in figures 3(a) and 4. When $\Delta = 1$, the power in $g^{(2)}(\tau)$ is smallest, so the feedback produces an oscillation with much more power than would have been there originally. As the detuning is increased, the power in the $g^{(2)}(\tau)$ oscillation increases again, with a different phase.

The model used in this case is the semi-classical description discussed in section 2.4. Two lossy oscillators are coupled at the vacuum-Rabi frequency. After the numerical solution comes to a steady state, energy is removed from the cavity oscillator. The amount of energy to remove is dictated by the $g^{(2)}(\tau = 0)$ value of the data for a given set of experimental parameters. The system is then allowed to re-evolve to the steady state. The energy exchange in the model system can be halted by changing the drive of the system at a given time. Detunings are added as described in equations (11) and (12). The barred region of figure 8 corresponds to a spread in values of the cavity–laser detuning of $\Theta = [-0.2\ 0.2]$. The model prediction diverges around $\Delta = 1$, which corresponds to the region where the power in $g^{(2)}(\tau)$ is minimal and the feedback produces much more power.

The asymmetry in the data is due to the non-zero value of Θ, which then results in a larger system response for one sign of Δ.

5. Conclusion

We have explored a novel quantum feedback technique. Our experiment is the first to use the knowledge gained from a quantum measurement to actively alter the dynamical evolution of the system [5].

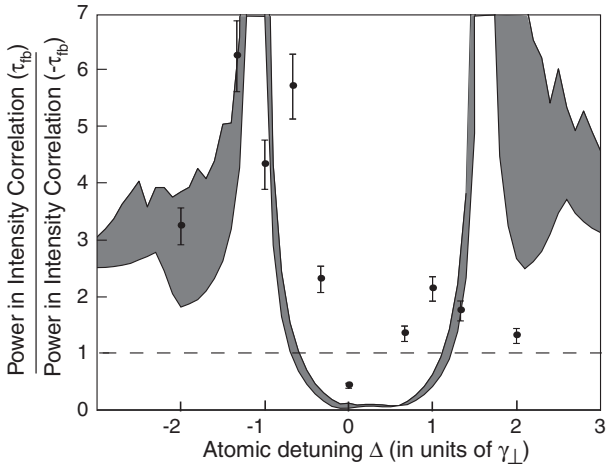

Figure 8. Power in the suppressed region of $g^{(2)}(\tau)$, normalized by the power in the same region at $g^{(2)}(-\tau)$. The grey area is theory and the range is given by the range of cavity detunings, $\Theta = [-0.2\ 0.2]$. The broken line corresponds to the value where the power in the suppressed region is equal to the power with no feedback.

The detection of single quanta triggers the quantum feedback which alters the intensity driving the system. The feedback can stop the evolution of the system into a new steady state. During the time that the driving intensity is altered, the likelihood that the system will emit a photon is constant. The system resides in a new steady state during this time. When we return the drive of the system to its original value, the system evolves with the same amplitude and parity that it would have without the feedback step. By timing our feedback to occur after a single quanta has been emitted from the system, we are able to stop the dynamic evolution which was initiated by the photodetection.

The feedback degrades in the presence of detuning, and with a range of detunings present in the cavity the observed suppression is a collective effect. Although the applied step is too large for atoms with a large detuning, it is too small for atoms with no detuning and the sum of these effects results in the suppression observed in the resonant case.

We explored the sensitivity of the system to the atom–cavity detuning and found that, by including the spread in Doppler detunings in the model, it agrees quantitatively with the data. The presence of detuning prevents perfect feedback as the system has four variables and the control protocol only two: amplitude and delay time. Future work will require extra parameters that can come from an optical lattice beam that captures the atoms in the cavity [31].

Acknowledgments

We would like to thank P R Rice and H M Wiseman for useful discussions. We would like to acknowledge the interest and help on this work from S Metz, C Pancake and J Reiner. The work supported by NSF and NIST.

References

[1] Foster G T, Orozco L A, Castro-Beltran H M and Carmichael H J 2000 *Phys. Rev. Lett.* **85** 3149
[2] Foster G T, Smith W P, Reiner J E and Orozco L A 2002 *Phys. Rev.* A **66** 033807
[3] Mielke S L, Foster G T and Orozco L A 1998 *Phys. Rev. Lett.* **80** 3948
[4] Foster G T, Mielke S L and Orozco L A 2000 *Phys. Rev.* A **61** 053821
[5] Smith W P, Reiner J E, Orozco L A, Kuhr S and Wiseman H M 2002 *Phys. Rev. Lett.* **89** 133601
[6] Reiner J E, Smith W P and Orozco L A 2003 *Phys. Rev.* A, submitted
[7] Carmichael H J, Castro-Beltran H M, Foster G T and Orozco L A 2002 *Phys. Rev. Lett.* **85** 1855
[8] Rempe G, Thompson R J, Brecha R J, Lee W D and Kimble H J 1991 *Phys. Rev. Lett.* **67** 1727
[9] Yamamoto Y, Imoto N and Machida S 1986 *Phys. Rev.* A **33** 3243
[10] Haus H A and Yamamoto Y 1986 *Phys. Rev.* A **34** 270
[11] Shapiro J H, Saplakoglu G, Ho S T, Kumar P, Saleh B E A and Teich M C 1987 *J. Opt. Soc. Am.* B **4** 1604
[12] Sánchez Mondragón J J, Narozhny N B and Eberly J H 1983 *Phys. Rev. Lett.* **51** 550
[13] Lugiato L A 1984 *Progress in Optics* vol 21, ed E Wolf (Amsterdam: North-Holland) p 69
[14] Carmichael H J, Brecha R J and Rice P R 1991 *Opt. Commun.* **82** 73
[15] Reiner J E, Smith W P, Orozco L A, Carmichael H J and Rice P R 2001 *J. Opt. Soc. Am.* B **18** 1911
[16] Mandel L and Wolf E 1995 *Optical Coherence and Quantum Optics* (New York: Cambridge University Press)
[17] Carmichael H J 1986 *Phys. Rev.* A **33** 3262
[18] Drummond P D 1991 *IEEE J. Quantum. Electron.* **17** 301
[19] Brecha R J, Rice P R and Xiao M 1999 *Phys. Rev.* A **59** 2392
[20] Xiao M, Kimble H J and Carmichael H J 1987 *Phys. Rev.* A **35** 3832
[21] Brecha R J, Orozco L A, Raizen M G, Xiao M and Kimble H J 1995 *J. Opt. Soc. Am.* B **12** 2329
[22] Mielke S L, Foster G T, Gripp J and Orozco L A 1997 *Opt. Lett.* **22** 325
[23] Raizen M G, Thompson R J, Brecha R J, Kimble H J and Carmichael H J 1989 *Phys. Rev. Lett.* **63** 240
[24] Zhu Y, Gauthier D J, Morin S E, Wu Q, Carmichael H J and Mossberg T W 1990 *Phys. Rev. Lett.* **64** 2499
[25] Gripp J, Mielke S L, Orozco L A and Carmichael H J 1996 *Phys. Rev.* A **54** R3746
[26] Gripp J, Mielke S L and Orozco L A 1997 *Phys. Rev.* A **56** 3262
[27] Rosenberger A T, Orozco L A, Kimble H J and Drummond P D 1991 *Phys. Rev.* A **43** 6284
[28] Carmichael H J and Sanders B C 1999 *Phys. Rev.* A **60** 2497
[29] Clemens J P and Rice P R 2000 *Phys. Rev.* A **61** 063810
[30] Raizen M G, Orozco L A, Xiao M, Boyd T L and Kimble H J 1987 *Phys. Rev. Lett.* **59** 198
[31] Terraciano M L, Smith W P and Orozco L A 2003 *CLEO-QELS 2003 Conf. Program* QTuG6 (Washington, DC: Optical Society of America)